Journal of Sustainable Bioenergy Systems, 2026, 16(4), 101-118
https://www.scirp.org/journal/jsbs
ISSN Online: 2165-4018
ISSN Print: 2165-400X

Influence of HFO Operating Temperature on the Performance of Centrifugal Separators in a Mini Thermal Power Plant in a Sahelian Climate: Case of the Ouaga East Plant

Hassime Guengané[1,2*], Souleymane Ramdé[1], Myriam J. A. D. Millogo[1,3], Thierry S. M. Ky[2], Sié Kam[2], Dieudonné Joseph Bathiébo[2]

[1]Multidisciplinary Research Laboratory in Engineering Science (LMRSI), Ecole Polytechnique de Ouagadougou, Ouagadougou, Burkina Faso
[2]Renewable Thermal Energies Laboratory (LETRE), Université Joseph KI-ZERBO, Ouagadougou, Burkina Faso
[3]Institut Supérieur d'Études de la Protection Civile (ISEPC), Ouagadougou, Burkina Faso
Email: *hassime.guengane@epo.gov.bf

How to cite this paper: Guengané, H., Ramdé, S., Millogo, M.J.A.D., Ky, T.S.M., Kam, S. and Bathiébo, D.J. (2026) Influence of HFO Operating Temperature on the Performance of Centrifugal Separators in a Mini Thermal Power Plant in a Sahelian Climate: Case of the Ouaga East Plant. *Journal of Sustainable Bioenergy Systems*, **16**, 101-118.
https://doi.org/10.4236/jsbs.2026.164006

Received: September 5, 2026
Accepted: November 8, 2026
Published: November 11, 2026

Copyright © 2026 by author(s) and Scientific Research Publishing Inc.
This work is licensed under the Creative Commons Attribution International License (CC BY 4.0).
http://creativecommons.org/licenses/by/4.0/
Open Access

Abstract

The Ouaga East thermal power plant uses heavy fuel oil (HFO), which requires preheating before injection into the centrifugal separators. Given the climatic environment, the plant experiences large daily ambient temperature variations ranging from 23˚C to 41˚C, with peaks often reaching 45˚C. Consequently, a fixed setpoint temperature of 95˚C leads to dangerous exceedances of the safety limit (>98˚C) in the afternoon and reduced separation efficiency at night. In this study, we propose an adaptive control strategy in which the setpoint is modulated in real time and maintained between 92˚C and 98˚C, with a simulation duration of 48 h. The thermal model is validated with an average RMSE of 1.09˚C, a bias of −0.14˚C, and an R^2 of 0.788. The results show that the HFO temperature is maintained within the optimal range during the simulation time, versus 77.6% for the fixed setpoint. Moreover, the separation efficiency remains unchanged. A deterministic economic analysis shows an annual gain of €32,449 (21.3 million FCFA) through energy savings (12.85%), reduced maintenance (46%), and avoided production losses (41.15%). A Monte Carlo simulation yields an average gain of €19,701 with a 90% confidence interval. The required investment is less than €4000, resulting in a payback period of less than one year. Adaptive control is therefore a simple, robust, and immediately cost-effective solution for improving the performance and safety of thermal power plants in Sahelian climates.

Keywords

Sahelian Climate, Centrifugal Separator, Heavy Fuel Oil (HFO), Adaptive Control, Separation Efficiency

1. Introduction

Like other West African countries, Burkina Faso's electricity supply is largely ensured by thermal power plants, especially during the dry season when hydroelectricity drastically decreases. The Kossodo thermal power plant (Ouagadougou), with a nominal capacity of 112.7 MW, covers nearly 73.86% of the energy demand of the Ouagadougou Regional Consumption Centre (CRCO) [1] [2]. It operates mainly on heavy fuel oil (HFO) because of its lower cost compared to diesel [1] [2]. However, the use of HFO under the sahelian climate conditions of Ouagadougou presents specific challenges related to the large variations in ambient temperature, which directly affect fuel viscosity and consequently the performance of treatment systems, namely centrifugal separators [3] [4]. Indeed, HFO contains impurities (water, salts, solid particles) that must be removed by centrifugal separators before injection into the engines in order to protect the injectors and internal components [5]. The efficiency of this separation strongly depends on the viscosity of the HFO, which itself is a function of temperature. Generally, preheating reduces viscosity and improves separation, up to a certain temperature threshold. Manufacturers recommend treatment temperatures of about 98˚C for standard HFOs, with an upper limit set by the flash point. The regulatory minimum flash point of HFOs is 60˚C [6] [7], with a safety margin of 10˚C. Below 60˚C, the viscosity becomes too high, separation is incomplete, and the risk of fouling increases. Above 98˚C, there is a fire risk and rupture of the purifier's hydraulic seal.

Ambient temperatures in Ouagadougou can vary from 23˚C at night to over 39˚C during the day, with heat peaks reaching 44˚C from March to June. These variations change the preheating requirements for HFO. In most power plants, the preheating setpoint of 98˚C is fixed for nominal operating conditions. This fixed setpoint is often unsuitable for diurnal fluctuations: in the afternoon, the high ambient temperature causes the HFO temperature to exceed 98˚C (safety risk); at night, the HFO can drop below 85˚C, reducing separation efficiency. At the Ouaga East thermal power plant, operating reports indicate recurrent separator failures that often lead to the shutdown of 1 out of 3 separators for more than one month [1]. These reports also mention recurrent failures of separation discs, bearings, seals, excessive sludge deposits, and costly maintenance, without a clear link to the thermal regulation strategy.

Recent scientific literature extensively addresses the viscosity and treatment temperature aspects of HFO. Although the studies conducted focus more on temperate or maritime climates where the main problem is heating in cold weather, the following lessons can be drawn:

Albin Fransson and Peter van der Brug in 2023 [8] investigated the systematic optimization of an existing preheating system. Their work examined the feasibility of replacing a 5000 cSt fuel with a 74,500 cSt fuel. The results showed that optimization of the preheating system, with the addition of an additional heat exchanger, is necessary to maintain efficiency as temperatures increase. Lei Zhou *et al.* [9] conducted a study on the effects of HFO and diesel properties on spray and combustion characteristics under operating conditions of a two-stroke marine engine. The performance of the fuels was studied under different ambient pressures, ambient temperatures, and other parameters. It was found that the combustion performance of HFO is sensitive to activation energy only at high engine speeds, and that ambient temperature and fuel temperature have negative effects on the Sauter mean diameter (SMD) distribution.

An experimental study by Jia Deng *et al.* [10] on the effect of ambient temperature on the macroscopic spray characteristics of low-sulfur HFO shows that ambient temperature has a negligible effect on spray penetration and cone angle, unlike ambient air density, which has a major impact. A numerical study conducted by Yousefifard *et al.* [11] highlights the effect of back pressures and ambient temperatures in the separator chamber on the spray characteristics of non-reactive HFO injected at high pressure. High ambient temperatures increase the spray penetration length regardless of the back pressure value in the chamber. Xiao Yu Chen *et al.* [12] examine the combustion characteristics of droplets of a mixture of HFO with 10% - 30% methanol. They find that the ignition delay and droplet lifetime of HFO and methanol/HFO decrease with increasing ambient temperature. Viktor Genkulov [13] studied the influence of HFO and MFP-HFO preparation modes on the operational reliability of engines. The results indicate that controlling both the separation temperature (98˚C) and the flow rate (70%) significantly reduces the probability of seizing on cylinder liners. The work of Zobayer Eusufzain *et al.* [14] focused on optimizing the efficiency of HFO separators in oil systems. This study shows that the HFO inlet temperature and the bowl rotation speed have a positive impact on separator performance. Noor Basheer Mohamed *et al.* [15] investigated possibilities for improving fuel properties and combustion systems in marine engines and boilers. For this, light diesel (LD) was mixed with heavy diesel (HD) to reduce fuel viscosity, and a mixture of 50% LD and 50% HD was also prepared. Evaluation of burner performance and exhaust emissions when heating the fuel to 50˚C, 70˚C, and 90˚C showed that the thermal efficiency of the LHD fuel is directly proportional to temperature, without addressing the critical preheating temperature which depends on flow rate and fuel viscosity. The work of Saleh, S. A. A. *et al.* [16] focused on improving the performance of a heat exchanger used as an exhaust gas heat recovery device to preheat heavy fuel oil in a brick factory. The HFO inlet temperature to the heat exchanger was set at 40˚C; therefore, they did not consider ambient temperature fluctuations in their evaluation. The study by Stewart *et al.* (2026) [17] quantified the operational gains resulting from a systematic optimization of preheating and separation. They achieved a 7.7% reduction in specific fuel consumption and a 43% decrease in unplanned engine shut-

downs. These results validate an economic model with a payback period of less than five months for the installation of precise temperature control systems. In his PhD thesis, Kontoulis [18] investigated CFD modeling of HFO flow and combustion in marine engines. He emphasized the thermophysical properties of the fuel and the effect of HFO preheating on spray development.

In summary, very few studies have examined the risk of overheating associated with high ambient temperatures. Moreover, economic analyses of the potential gains from adaptive control are rare, particularly in the African context. Recent work confirms that a higher temperature improves the efficiency of HFO separators, but this practice is strictly constrained by safety limits (flash point) and operational limits (fuel aging, energy consumption) to ensure safe and sustainable operation.

Thus, this work aims to answer the following question: how can the HFO inlet temperature to the centrifugal separators of a Sahelian thermal power plant be optimized to maintain both high separation efficiency and safety, while quantifying the economic benefits? To address this, we developed a validated simplified thermal model and then simulated fixed and adaptive control strategies over a representative climatic cycle for the city of Ouagadougou. Performance indicators such as HFO temperature, centrifugal separator separation efficiency, and time spent outside limits were determined. We also estimated annual gains and investment profitability using deterministic economic analysis and uncertainty analysis via the Monte Carlo approach. Finally, we propose practical recommendations for the Ouaga East plant and discuss the limitations and perspectives of this work.

2. Materials and Methods

2.1. Description of the Site and Equipment

The study was conducted at the Ouaga East thermal power plant in Kossodo (Burkina Faso). The facility comprises eleven (11) generator sets of different brands (MAN B & W, DEUTZ, WARTSILA) with nominal powers ranging from 3.8 to 18.9 MW. They are equipped with centrifugal separators of the purifier type (Alfa Laval, model PX G) [1]. These separators treat the HFO before injection into the engines [19]. The preheating system consists of electric heaters immersed in the supply circuit, regulated by a programmable logic controller (PLC) that maintains a temperature setpoint at the separator inlet. The viscosity of the HFO varies according to its quality; the more viscous the HFO, the higher the required heating temperature. Table 1 summarizes the physical constant values proposed by our previous work [1]:

Table 1. Physical characteristics of the HFO at the Ouaga East plant.

Kinematic viscosity at 50˚C (mm²/s)	Kinematic viscosity at 98˚C (mm²/s)	Density (kg/m³)	Average water content (%)	Nominal volumetric flow rate (m³/s)
163.11	30.02	945.57	1.2	0.070

Figure 1 shows two images of the site, namely a separator and the unloading device.



(a) (b)

Figure 1. Images of the components of the Kossodo thermal power plant: (a) Separator; (b) unloading device).

2.2. Modeling of the Thermal Behavior of HFO

To model the impact of ambient temperature variations on the HFO temperature downstream of the heater, we use a simplified approach that relates the HFO temperature (T) at the separator inlet to the preheater setpoint temperature (T_p) and to the ambient temperature (T_a). The equation adopted is:

$$T(t) = T_p(t) + \alpha\left[T_a(t) - T_{a,ref}\right] \quad (1)$$

The setpoint temperature T_p is chosen to achieve an ideal viscosity for centrifugal separation.

The coefficient α (ranging from 0.2 to 0.8) is an empirical parameter that aggregates the influence of thermal losses from the installation (piping, equipment) on the fuel [20]. $\alpha = 0.2$ corresponds to a slow increase in the fluid temperature as the outside temperature decreases [21]. The reference ambient temperature $T_{a,ref}$ is the average ambient air temperature for a typical year. Its value is 34.75 [22].

2.3. Climatic Profile

The ambient temperature of the city of Ouagadougou was modeled by a sinusoidal function with a period of 24 hours, representative of the monthly averages during the hot season in Ouagadougou:

$$T_a(t) = T_{a,ref} + \frac{A}{2}\sin\left[\frac{2\pi t}{86400} + \phi\right] \quad (2)$$

With,

A is the peak-to-peak amplitude, with a value of 21.3˚C [23]; ϕ is the phase shift. It is obtained from the following formula: $\phi = \frac{\pi}{2} - \frac{2\pi}{86400}\left(t_{pic} - t_0\right)$

where t_{pic} and t_0 are the time at which the temperature peak is observed and the initial time, respectively.

2.4. Performance Model of the Separator

We use Andrade's law [24] [25] to model the efficiency of solids removal by the centrifugal separator as a function of the dynamic viscosity of the HFO, which depends on temperature:

$$\mu(T) = A_\mu \exp\left(\frac{B_\mu}{T(^\circ\mathrm{C}) + 273.15}\right) \tag{3}$$

The parameters $A_\mu = 2.49\times10^{-4}$ cSt and $B_\mu = 4311$ K were calculated from the kinematic viscosity values in **Table 1** above. The value of the constant B_μ is low. This indicates a viscosity that varies less rapidly with temperature. Indeed, for the same temperature increase, the viscosity drop is more moderate. In other words, the HFO used at the studied plant is less thermally sensitive, and therefore heavier.

❖ The separation efficiency η (fraction of solids) is given by [14] [26]:

$$\eta(T) = \begin{cases} 0.99 & \text{if } \mu \le \mu_{ref} \\ 1 - \left(\dfrac{\mu - \mu_{ref}}{\mu_{\max} - \mu_{ref}}\right)^n (1 - \eta_{\min}) & \text{if } \mu_{ref} \prec \mu \prec \mu_{\max} \\ \eta_{\min} & \text{if } \mu \ge \mu_{\max} \end{cases} \tag{4}$$

This formulation reflects the following principle:

❖ If $T \prec 95^\circ\mathrm{C} \rightarrow \mu \succ 30$ cP $\rightarrow$ the separation efficiency begins to decline.

❖ If $T \ge 95^\circ\mathrm{C} \rightarrow \mu \le 30$ cP $\rightarrow$ maximum efficiency (99%).

This highlights the value of adaptive control when it is cold ($T_{a,\min}$), the fixed strategy causes T to drop below 95˚C, thereby degrading efficiency, whereas the adaptive strategy corrects this phenomenon.

❖ Water separation efficiency:

The water removal efficiency function was calibrated on eleven (11) measurements of water content before/after the separator, performed at temperatures ranging from 55˚C to 110˚C in 5˚C increments. A logistic regression was used to estimate a half-efficiency temperature of 75˚C and a slope of 0.3 [14] [24]. Equation (5) provides the mathematical model used. Water evaporates more effectively as temperature increases.

$$\eta_e = \frac{1}{1 + \exp\left(-0.3\times(T - 75)\right)} \tag{5}$$

❖ **Fire Risk**

The fire risk is modeled by a logistic function defined by Equation (6), centered on the flash point of HFO, measured at 98˚C, with a slope of 0.8 [27].

$$\eta_{inc} = \frac{1}{1 + \exp\left(-0.8\times(T - 98)\right)} \tag{6}$$

❖ **Hydraulic Risk**

The hydraulic risk is modeled by Equation (7). It is centered on 105˚C, the maximum service temperature for seals and the lubrication system, with a slope of 0.8 [28] [29]. This limit is consistent with the minimum viscosity range required for the pumps.

$$\eta_{hyd} = \frac{1}{1+\exp\left(-0.8\times\left(T-105\right)\right)} \tag{7}$$

The overall separation efficiency is the product of the two efficiencies calculated above.

2.5. Control Strategies

Two strategies were compared:

- Fixed setpoint: $T_{sat} = 95^{\circ}\text{C}$ (commonly used value).
- Adaptive control: the setpoint is adjusted in real time according to the ambient temperature:

$$T_{set}\left(T_a\right) = \max\left(T_{\min}, \min\left(T_{\max}, T_{opt} - k\left(T_a - T_{a,ref}\right)\right)\right) \tag{8}$$

with, $T_{opt} = 95^{\circ}\text{C}$, $T_{a,ref} = 34.75^{\circ}\text{C}$, $k = 0.34$, $T_{\min} = 85^{\circ}\text{C}$ et $T_{\max} = 98^{\circ}\text{C}$.

Note that the operating band is the temperature interval [30]: $\left[85^{\circ}\text{C}; 98^{\circ}\text{C}\right]$.

The parameter k is the adaptation gain of the setpoint law. It results from a constrained optimization that maximizes the average efficiency while ensuring that the HFO temperature remains within the safe and efficient zone. For example, k equal to α cancels the influence of the ambient (perfect compensation).

We will retain two temperature thresholds:

✓ a fire safety threshold ($98^{\circ}\text{C} \prec T \prec 105^{\circ}\text{C}$, dangerous);

✓ a process safety threshold ($T \succ 105^{\circ}\text{C}$, risk of hydraulic seal failure).

2.6. Numerical Simulation

We used Python version 3.11 for the simulation. The simulation period is 48 hours, discretized into 2000 points. For each of the two control strategies, we calculated the following quantities:

✓ the HFO temperature at each time step;

✓ the instantaneous separation efficiency of the HFO by the centrifugal separators;

✓ the maximum temperature reached during preheating;

✓ the fraction of time spent outside the range.

2.7. Economic Analysis

2.7.1. Scope and Basis for Conversion and Assumptions to Be Retained

Table 2 defines the scope of the economic study.

Energy and maintenance gains are calculated at the fuel treatment line level, avoided production is calculated at the entire power plant level, and the investment must be allocated to the treatment line (adaptive control system).

Table 2. Scope of the study.

Parameter	Consistent scope	Justification
Fuel flow rate	Fuel treatment line (preheater + separator)	Used to calculate the HFO heating power. This is not the flow rate of the entire power plant, but that of the fuel line.
Preheater load	Fuel treatment line	$\Delta T = T_{set} - T_e$ represents the preheating energy of HFO before separation.
Investment	Fuel treatment line	Adaptive control, sensors, valves, and automation systems concern the preheater/separator, not the entire power plant.
Avoided production	Entire power plant	A major failure of the fuel line can cause shutdown of the power plant. The production loss is therefore calculated based on the power plant capacity.
Maintenance savings	Fuel treatment line	These costs are directly related to separation quality and fouling of the fuel line.

We have retained €26,000/year for a 100% reduction in out-of-band time, *i.e.*, €260/year per percentage point of reduction in out-of-band time. The 80% assumption applies to the total failure cost (lost production + restart).

2.7.2. The Variables Considered for the Economic Analysis

The economic analysis focused on energy savings, maintenance, and production losses:

❖ **Energy savings:** this is the difference in electrical energy consumed by the preheater. It is obtained by performing the following successive calculations:

✓ the instantaneous power: $P = D_m C_p \left(T_{set} - T_e\right)$, where T_e is the HFO inlet temperature, close to T_a;

✓ the fixed power: $P_{fixe} = D_m C_p \left(T_{set,\,fixe} - T_a\right)$

✓ the adaptive power: $P_{ad} = D_m C_p \left(T_{set,\,ad} - T_a\right)$

✓ instantaneous power savings (in W): $P_{eco} = P_{fixe} - P_{ad}$

✓ energy saved over the simulation period (48 h): $E_{eco} = P_{eco} \dfrac{t}{3600}$

✓ projection over one year (8760 h): $E_{eco,an}\left(\text{kWh}\right) = p \times f_{ex} \times \dfrac{E_{eco}\left(\text{Wh}\right)}{1000}$ where f_{ex} is the extrapolation factor given by: $f_{ex} = 8760/48 = 182.5$ and p is the production cost per kWh of electricity.

Table 3 below presents the production cost per kWh of electricity for different sources [31].

Table 3. Average production cost per kWh of electricity.

Sources	Solar photovoltaic	Hydroelectricity	Interconnection (import)	Thermal (Diesel/Fuel)
Average production cost (FCFA)	15	39	64	105 - 160

For the simulation, we set the production cost of electricity at 132 FCFA per kWh, *i.e.*, 0.2 €/kWh.

❖ **Maintenance:** reduction in the frequency of unloading operations (fixed sav-

ing of 6,558,294 FCFA/year, *i.e.*, 10,012€/year), savings on filters and seals (2,278,768 FCFA/year, *i.e.*, 3479€/year) and on injectors and separation discs (3,122,242 FCFA, *i.e.*, 4767€/year), proportional to the reduction in time spent outside the optimal zone.

- ✓ **Avoided production losses:** this involves avoiding a major failure of 4 hours per year (lost production + restart cost). We set the average selling price per kWh at 150 FCFA, *i.e.*, 0.23€/kWh. Our previous work [1] established a downtime rate of 30.3%, corresponding to a total downtime of 2654.28 hours per year.
- ❖ It is estimated that the probability of a major failure is reduced by 80% thanks to adaptive control.

The following steps are carried out to evaluate the losses:

- ✓ lost production (kWh) = nominal plant capacity*failure duration (hours);
- ✓ cost of lost production = lost production (kWh)*selling price per kWh;
- ✓ total cost of a major failure = Lost production cost + Restart cost;
- ✓ failure savings = total failure cost*risk reduction;
- ✓ annual savings = annual energy saving + unloading saving + filter saving + injector savings + failure savings.
- ✓ Payback period = expenses divided by the Monte Carlo average annual gain.

2.8. Monte Carlo Uncertainty Analysis

To account for the variability of economic parameters, a Monte Carlo simulation was performed:

- ➢ Number of draws: 10,000;
- ➢ Random seed: 42
- ➢ Outputs are expressed in €/year.

Dependency assumptions:

The purchase and sale prices are positively correlated $(\rho = 0.7)$; all other variables are independent. The out-of-band reduction is derived from the deterministic simulation and remains fixed in the baseline Monte Carlo.

The distributions used are presented in Table 4 below:

Table 4. Distributions used for the economic analysis.

Variable	Distribution	Parameters	Bounds
Purchase price of kWh (€/kWh)	Truncated normal	$\mu = 0.2; \sigma = 0.02$	$[0.06; 0.23]$
Sale price of kWh (€/kWh)	Truncated normal	$\mu = 0.23; \sigma = 0.02$	$[0.18; 0.28]$
Dependency	Gaussian copula	$\rho = 0.7$ on normal latent variables	—
Unloading gain	Lognormal	$\mu = \ln(26000); \sigma = 0.3$	Truncated [0; 26,000]
Filter gain	Lognormal	$\mu = \ln(26000); \sigma = 0.3$	—
Injector gain	Lognormal	$\mu = \ln(10000); \sigma = 0.3$	—
Risk reduction	Beta	$A = 8$, $b = 2$	mean = 0.80; standard deviation ≈ 0.12
Energy savings (kWh)	Deterministic	derived from the 48-h simulation	Normal with mean 20,848 kWh, σ = 10%

We will calculate the gains for each draw, then analyze the distribution (mean, standard deviation, percentiles).

3. Results and Discussion

3.1. Evolution of HFO Physical Parameters and Separation Efficiency

Figure 2 presents the evolution of the kinematic (cSt) and dynamic (cP) viscosities and the separation efficiency of the HFO as a function of the temporal evolution of the HFO temperature at the separator inlet. The viscosities decrease exponentially with fuel temperature, in accordance with the law in Equation (3). The threshold value of 30 cP is reached for a temperature of 62˚C. Below this value, flow becomes difficult, increasing pressure in the circuits and reducing atomization. Above 80˚C, viscosity decreases further but gains become marginal. These observations justify a minimum heating temperature around 70˚C to 80˚C to ensure good atomization without unnecessary overheating. Moreover, the water separation efficiency increases with temperature because settling is facilitated by the decrease in viscosity and the increase in the water/HFO density difference. It exceeds 90% around 85˚C. The solids separation efficiency exhibits non-monotonic behavior: almost constant at low temperatures $(\prec 60^{\circ}\mathrm{C})$ where high viscosity retains particles, it increases slightly then drops when viscosity becomes too low to trap solids. The overall efficiency is the geometric compromise of the two: it peaks around 80˚C then decreases slightly. This result shows that an excessively high temperature $(\succ 90^{\circ}\mathrm{C})$ no longer improves overall separation and can even degrade it, justifying a narrow target range.

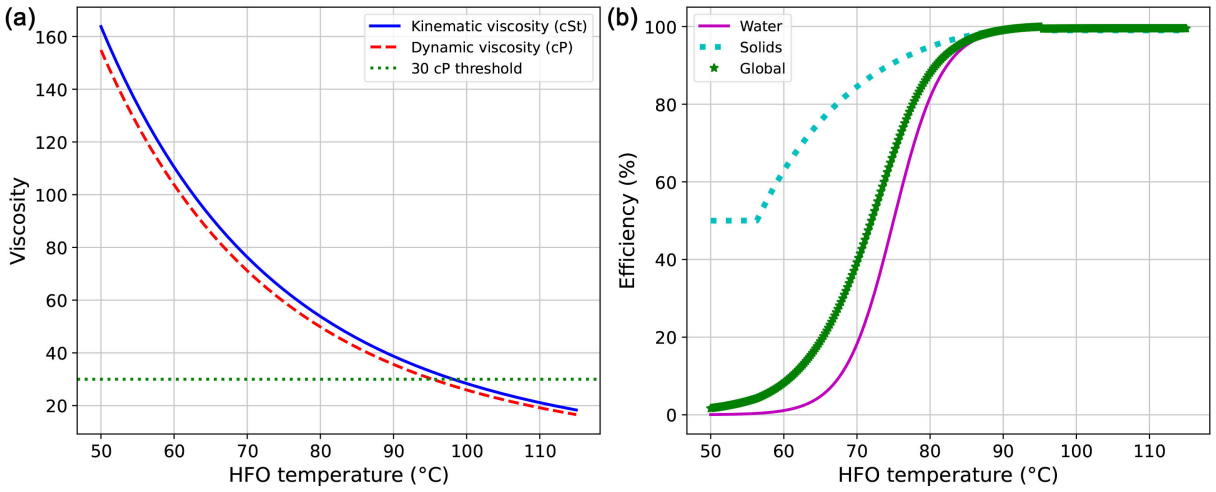


Figure 2. Separator performance curves: (a) HFO viscosity as a function of temperature; (b) Centrifugal separator performance.

3.2. Comparative Performance of Control Strategies

❖ **Operational risks and critical zones**

Before examining the impact of the control strategy on HFO separation effi-

ciency by the separators, Figure 3 presents the operational risks and critical zones to be considered for the analysis of the results. Thus, according to the HFO temperature zones, the following legend was adopted:

[50; 60], red: Very poor separation;

[60; 85], orange: Poor separation;

[85; 92], yellow: Acceptable separation;

[92; 98], light green: Optimal range;

[98; 105], dark orange: Fire hazard;

[105; 115], red: Fire + hydraulic hazard.

The separation risk is high at temperatures below 70˚C and decreases to a minimum around 85˚C - 90˚C. The hydraulic risk remains negligible up to 100˚C and then increases sharply as 105˚C is approached (partial vaporization, cavitation). The fire risk becomes significant above 95˚C and increases strongly after 98˚C. By superimposing the three curves, the zone of minimal risk is obtained between 85˚C and 98˚C, which corroborates the operating band. Beyond this range, fire risk dominates; below it, separation risk degrades fuel quality.

The overall efficiency curve alone could suggest that a temperature of 80˚C is optimal. However, the mapping of the zones reveals that the safe operating range is shifted toward 85˚C - 95˚C. This illustrates the compromise between performance and safety: the operational optimum is not the maximum efficiency, but the point where risks remain acceptable while maintaining sufficient efficiency.

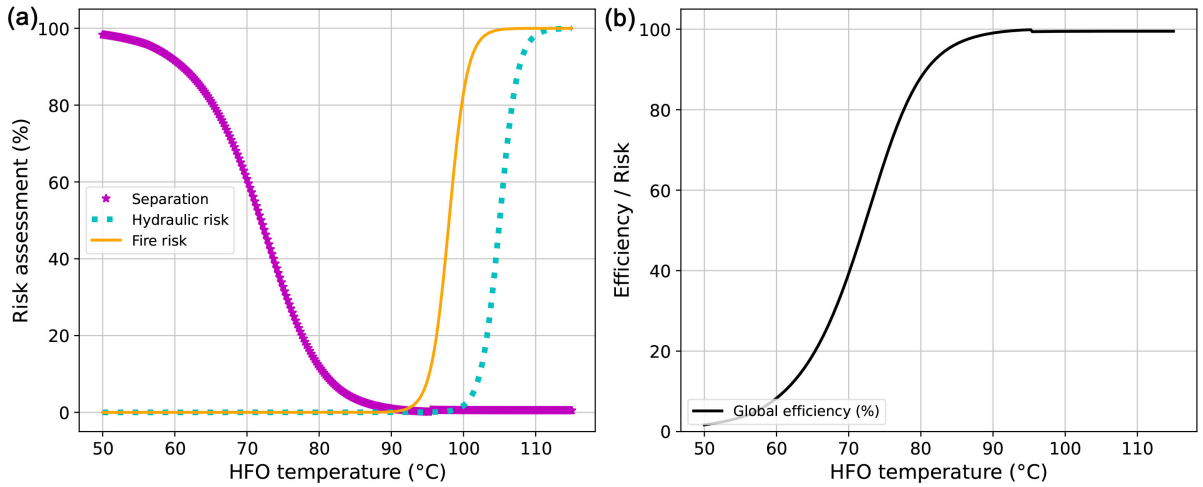


Figure 3. Operational performance zones: (a) Operational risks, (b) Critical operating zones.

❖ Control strategies

Figure 4(a) reproduces the sinusoidal profile of the ambient temperature in the city of Ouagadougou, with a minimum of 22˚C around 6 a.m. and a maximum of 44.5˚C in the afternoon. This 22.5˚C variation has a direct impact on the HFO temperature, because the heating system must compensate for thermal losses and the variation in inlet temperature. Figure 4(b) presents the evolution of the HFO

temperature during the first 12 hours of the day according to the two control strategies presented in Section 2.5. The fixed regime maintains a setpoint of 95˚C, but when the ambient temperature exceeds 40˚C, the HFO temperature exceeds 98˚C and enters the fire risk zone. The adaptive control then lowers the setpoint to keep the temperature below 98˚C, while remaining above 92˚C. This anticipation is crucial to avoid dangerous excursions while maintaining good separation efficiency. The slight time lag between the ambient temperature and the adaptive control response illustrates the time constant of the heating system.

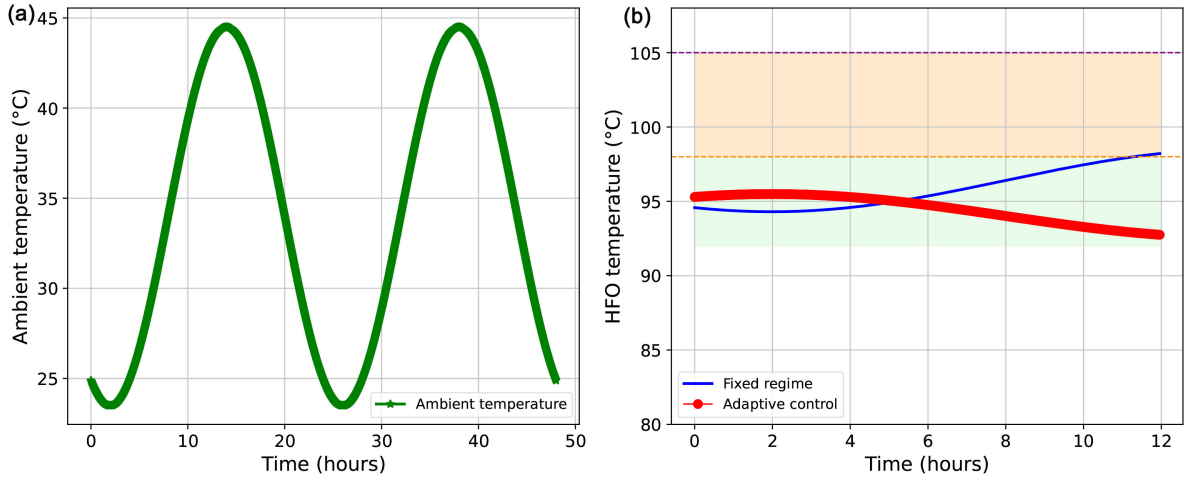


Figure 4. Temperature profile: (a) Ambient temperature; (b) Zoom of the HFO temperature over the first 12 hours.

To better observe the impact of adaptive control, we track the HFO temperature profile over 48 h in **Figure 5**. With the fixed control model, the HFO temperature remains almost at 95˚C, but regularly exceeds 98˚C during hot periods, thus entering the fire risk zone. The adaptive model curve follows a lower and more stable trajectory: it remains within the optimal zone and never exceeds 98˚C, even when the ambient temperature is high.

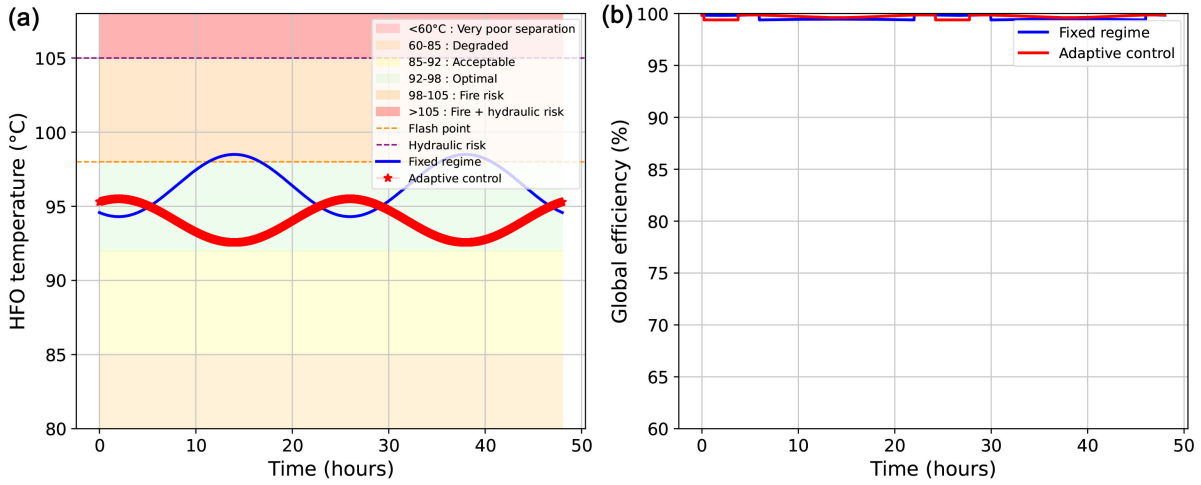


Figure 5. Control strategies: (a) Comparison of control strategies; (b) Setpoint evolution.

As an illustration, Table 5 presents the performance indicator values for the two control strategies. The efficiency of the adaptive control is more stable. Indeed, the fixed strategy maintains a higher average temperature of 96˚C, which promotes better water/solids separation in steady state. However, this average conceals a major problem: the fixed control spends 22.4% of the time outside the safety zone, exposing the installation to risks of fire, equipment degradation, and unplanned shutdowns.

Table 5. Performance indicators.

Indicator	Fixed control (setpoint 95˚C)	Adaptive control (k = 0.34)
Average HFO temperature (˚C)	96.4	94.0
Standard deviation of fluctuations (˚C)	1.49	1.04
Average separation efficiency (%)	99.6	99.7
Time outside optimal zone (%)	22.4	0.0

These results clearly demonstrate the advantage of adaptive control over a fixed setpoint in a Sahelian climate with high thermal variability. The optimal temperature range [92˚C - 98˚C] is respected almost throughout the entire 48 hours with the proposed strategy, compared with less than 80% with the fixed setpoint. This gain is directly related to the compensation of the ambient influence by the term $-k\times\left(T_a - T_{a,ref}\right)$. The value $k = 0.2$ (equal to the coefficient α) effectively cancels the sensitivity to variations in T_a, as shown by the equation:

$$T = T_{opt} + \left(\alpha - k\right)\left(T_a - T_{a,ref}\right) = T_{opt}$$

in the zone where the limits are not active. This theoretical result is confirmed by the low residual variability (standard deviation of 1.04˚C versus 1.49˚C for the fixed setpoint). However, it should be noted that both strategies exhibit almost the same average efficiency.

3.3. Deterministic Economic Analysis (Annual)

The annual economic assessment of adopting the adaptive control we propose is recorded in Table 6. The savings are estimated from the simulation results and the unit costs of electricity per kWh provided in Table 3. Note that this study covers the three (03) separators of the thermal power plant.

Table 6. Estimated annual economic gains.

Item	Energy savings	Reduction in landfilling	Injector savings	Filter savings	Avoided production losses	Total
Annual Gain (€)	4170	2926	10,000	2000	13,353	32,449
%	12.85	9.02	30.82	6.16	41.15	100

The energy saving, although modest (4170€), results from the reduction of the setpoint during hot periods. The most significant gains are related to maintenance: reductions in unloading operations, filter replacements, and injector repairs. Finally, the avoidance of approximately one major failure per year, with a rate of 0.01159 failures/hour [1], yields 13,353€ annually. The annual total is therefore estimated at 32,449€. However, the initial investment required to adopt the adaptive control strategy (ambient temperature sensor and controller reprogramming) does not exceed 4000€, leading to a payback period of less than one year.

3.4. Uncertainty Analysis (Monte Carlo)

The Monte Carlo simulation (10,000 draws) yields a nearly normal distribution of annual gains. Figure 6 presents the histogram. The mean is 19,701€, the standard deviation is 1996€, and the 90% confidence interval is [16,224€; 22,778€]. Even in the most unfavorable scenario (5th percentile), the gain remains above 16,224€.

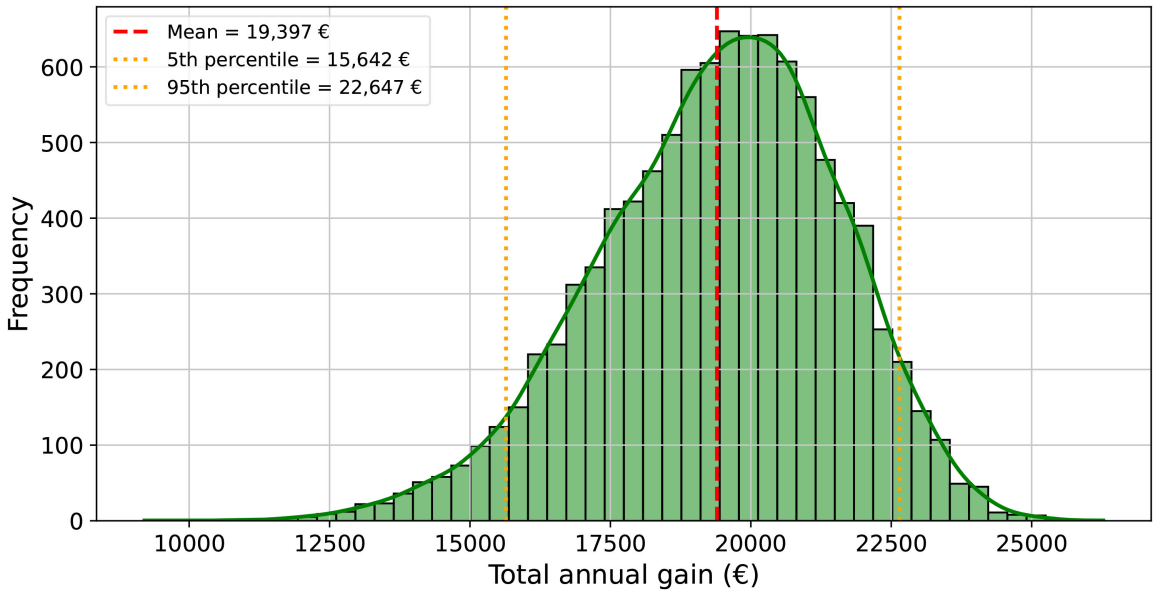


Figure 6. Distribution of total annual gains obtained by Monte Carlo.

Given the economic results obtained, the deterministic estimate is supported by the Monte Carlo analysis. The difference between the two values arises from the nonlinearity and the bounds applied to the distributions. The narrowness of the confidence interval (approximately ±14% around the mean) shows that economic uncertainties do not call into question the profitability of applying the strategy. Moreover, even the 5th percentile is four times higher than the investment cost.

Maintenance items (unloading operations, filters, injectors) account for the largest share of the gains. This suggests that the main impact of adaptive control is operational (reliability, availability) rather than energy-related. Of course, energy savings are not negligible, representing nearly 13% of the total gain.

3.5. Validation of the Thermal Model

The real data include 50 points recorded over 48 h, *i.e.*, a sampling interval of 58.8 min. Type K thermocouples $(\pm 1.1^{\circ}\mathrm{C})$, placed immediately upstream of the three centrifugal separators, measure the HFO temperature. The ambient temperature is measured directly on site in the shade. From the real measurements, the thermal coefficient α was calibrated by linear regression of $(T - T_{opt})$ as a function of $(T_a - T_{a,ref})$, then evaluated on 25 records not used for calibration. The simplified thermal model was validated with a mean RMSE of 1.09˚C, a bias of −0.14˚C, and an R^2 of 0.788˚C. These values indicate a very good agreement between the simulated model and the recorded values. These performances are excellent for such a simple model, and they justify its use for sizing the adaptive control.

However, the model has limitations mainly related to the system dynamics, because the instantaneous linear equation does not account for thermal inertia (delays, time constants), and to the climate model (the sinusoid used does not account for climatic variability such as winds and cloud cover). Figure 7 presents the validation curves.

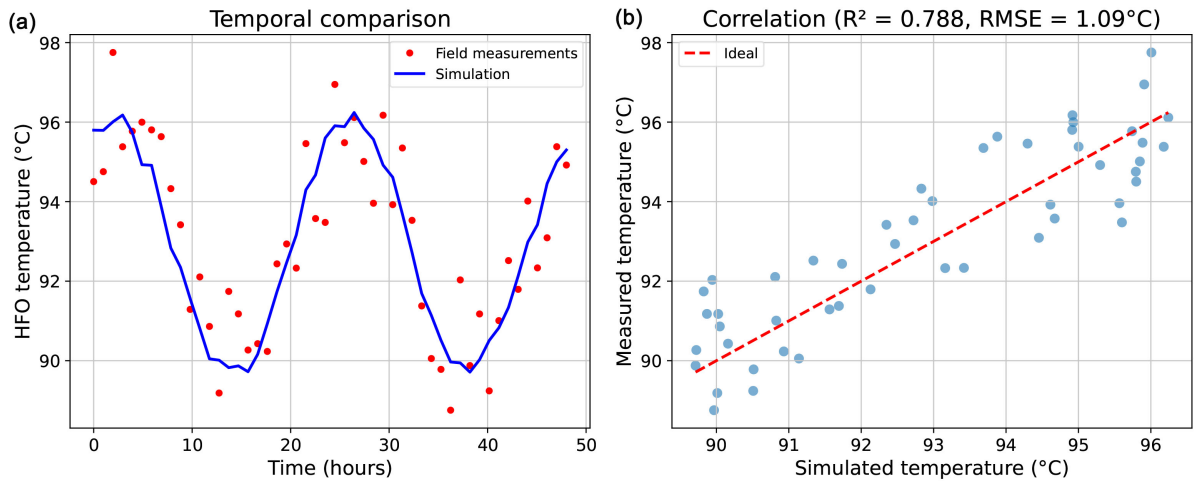


Figure 7. Model validation (a) temperature time series; (b) correlation between simulated and measured values.

4. Conclusions

The results obtained from this study demonstrate that an adaptive control strategy for the HFO inlet temperature in centrifugal separators makes it possible to maintain operation within the band $[85^{\circ}\mathrm{C}; 98^{\circ}\mathrm{C}]$, more specifically within the optimal safety and performance range $[92^{\circ}\mathrm{C}; 95^{\circ}\mathrm{C}]$, despite a Sahelian climate with high thermal variability. The adaptive control was simulated over 48 hours based on real climatic data from the city of Ouagadougou and compared to a fixed setpoint of 95˚C. The results show that the adaptive control does not aim to maximize instantaneous efficiency, but rather to optimize the overall operation of the plant while respecting safety and reliability constraints. Both strategies yield almost the same average efficiency, but the adaptive strategy ensures the absence of critical threshold exceedances and operational stability. The economic analysis, which fo-

cused on energy savings, maintenance reduction, and the avoidance of production losses, estimates a deterministic annual gain of 32,449€ (approximately 21.3 million FCFA). A Monte Carlo simulation with 10,000 draws confirms the economic robustness of the model, with an average gain of 19,701€ and a 90% confidence interval of [16,224€; 22,778€]. The investment required for the three separators of the power plant (sensors, reprogramming) is less than €12,000, yielding a payback period of less than one year (7 months and 9 days). The thermal model was validated with an RMSE of 1.09˚C and an R^2 of 0.788, indicating very good predictive capability despite its simplicity. It can therefore be concluded that adaptive control is a simple, robust, and immediately cost-effective solution for improving the performance, safety, and availability of thermal power plants using HFO in Sahelian climates.

As future work, this study could be applied to other Sahelian power plants. Additionally, predictive control using weather forecasts (24-hour ambient temperature) would make it possible to anticipate variations and smooth the setpoint.

Acknowledgements

The authors thank the management of the Kossodo thermal power plant (SONABEL) for access to technical data and for the fruitful discussions with the maintenance teams.

Author Contributions

Hassime Guengané: Writing—review & editing, Data curation, Conceptualization; Souleymane Ramdé: Writing—original draft, Supervision, Data curation, Conceptualization; Myriam J. A. D. Millogo: Writing—review & editing, Investigation, Formal analysis; Thierry Sikoudouin Maurice Ky: Software, Formal analysis; Sié Kam: Supervision, Project administration; Dieudonné Joseph Bathiébo: Validation, Supervision, Resources, Funding acquisition.

Conflicts of Interest

The authors declare no conflicts of interest regarding the publication of this paper.

References

[1] Guengane, H., Toure, A.A., Tougri, I., Ky, T.S.M., Kam, S. and Bathiébo, D.J. (2026) Failure Mode Analysis and Reliability Assessment of HFO Centrifugal Separators in a Thermal Power Plant: A Case Study of the Ouaga East (Kossodo) Power Plant, Burkina Faso. *Open Journal of Applied Sciences*, **16**, 2668-2681. https://doi.org/10.4236/ojapps.2026.168149

[2] IRENA (2023) Évaluation de l'état de préparation aux énergies renouvelables: Burkina Faso. https://www.irena.org/-/media/Files/IRENA/Agency/Publication/2023/Dec/IRENA_RRA_Burkina_Faso_2023_FR.pdf

[3] Prabhu, S. (n.d.) Centrifuge Fluid Heating Systems. Dolphin Centrifuge. https://dolphincentrifuge.com/fluid-heating-systems/

[4] Mateu-Royo, C., Mota-Babiloni, A., Navarro-Esbrí, J. and Barragán-Cervera, Á. (2021) Comparative Analysis of HFO-1234ze(E) and R-515B as Low GWP Alternatives to HFC-134a in Moderately High Temperature Heat Pumps. *International Journal of Refrigeration*, **124**, 197-206. https://doi.org/10.1016/j.ijrefrig.2020.12.023

[5] Klebert, S., Becker, K., Kocherscheidt, A., *et al.* (2026) Heavy Fuel Oil Treatment—Reliable Performance and Protection.

[6] ISO (2024) ISO 8217:2024—Products from Petroleum, Synthetic and Renewable Sources—Fuels (Class F)—Specifications of Marine Fuels (7e éd.). Organisation internationale de normalisation. 41 p. Comité technique: ISO/TC 28/SC 4.

[7] Li, W., Liu, R., Liu, Y., Wang, D., Shi, J. and Chen, J. (2020) Performance Evaluation of R1234yf Heat Pump System for an Electric Vehicle in Cold Climate. *International Journal of Refrigeration*, **115**, 117-125. https://doi.org/10.1016/j.ijrefrig.2020.02.021

[8] Fransson, A. and van der Brug, P. (2020) Systematic Optimisation of an Existing Fuel Oil Preheating System: Facilitating Replacement of 5000 cSt Oil with 74,500 cSt. University Essay/Thesis, Linnéuniversitetet, Institutionen för maskinteknik (MT). http://urn.kb.se/resolve?urn=urn:nbn:se:lnu:diva-96033

[9] Zhou, L., Shao, A., Wei, H. and Chen, X. (2017) Sensitivity Analysis of Heavy Fuel Oil Spray and Combustion under Low-Speed Marine Engine-Like Conditions. *Energies*, **10**, Article No. 1223. https://doi.org/10.3390/en10081223

[10] Deng, J., Yi, P., Li, T., Hong, S. and Chen, R. (2022) Complex Physicochemical Process of Low Sulfur Heavy Fuel Oil under High Temperatures and Pressures. *The Proceedings of the International Symposium on Diagnostics and Modeling of Combustion in Internal Combustion Engines*, **2022**, C1-2. https://doi.org/10.1299/jmsesdm.2022.10.c1-2

[11] Yousefifard, M., Ghadimi, P. and Nowruzi, H. (2015) Numerical Investigation of the Effects of Chamber Backpressure on HFO Spray Characteristics. *International Journal of Automotive Technology*, **16**, 339-349. https://doi.org/10.1007/s12239-015-0036-z

[12] Chen, X., Long, W., Wang, Y., Xiao, G., Dong, P., Wang, Z., *et al.* (2024) Experimental Investigation on Enhanced Combustion of Methanol/Heavy Fuel Oil by Droplet Puffing at Elevated Temperatures. *Scientific Reports*, **14**, Article No. 14525. https://doi.org/10.1038/s41598-024-64482-x

[13] Genkulov, V. (2026) Optimization of the Marine Fuel System (MGO/HFO, MFP-HFO, Separation): The Influence of Fuel Preparation Modes on Engine Reliability and Consumption. Preprint/Version 1, Engineering Archive (engrXiv). https://doi.org/10.31224/6908

[14] Eusufzai, Z. and Shil, S.K. (2024) Enhancing HFO Separator Efficiency: A Data-Driven Approach to Petroleum Systems Optimization. *International Journal of Scientific Interdisciplinary Research*, **5**, 261-300. https://doi.org/10.63125/2tzaap28

[15] Mohamed, N.B. and Saleh, A.M. (2025) Experimental Study of the Effect of Heating Diesel Fuel on Burner Performance and Emissions. *Journal of Advanced Research in Experimental Fluid Mechanics and Heat Transfer*, **19**, 44-45. https://doi.org/10.37934/arefmht.19.1.4455

[16] Saleh, S.A.A., Kadhim, Z.K. and Khalaf, K.A. (2024) An Experimental Study of Heating Heavy Fuel Oil by Hot Air Using Helical Fins in a Double-Pipe Heat Exchanger. *Journal of Advanced Research in Fluid Mechanics and Thermal Sciences*, **112**, 102-115. https://doi.org/10.37934/arfmts.112.2.102115

[17] Stewart, C., Alves, Z. and Hamilton, A. (2026) Optimization of Marine Fuel Preparation and Separation Processes for Enhancing Engine Reliability and Reducing Fuel

Consumption in Commercial Vessels [Preprint]. ResearchGate.

[18] Kontoulis, P. (2019) Computational Study and Optimization of Flow and Combustion Processes in Marine Engines Operating with Heavy Fuel Oil. Thèse de Doctorat (PhD Thesis), National Technical University of Athens (NTUA). https://phdtheses.ekt.gr/eadd/handle/10442/46257

[19] GEA Westfalia Separator (2010) Settings and Malfunctions: Separator with Self-cleaning Bowl, Type D 10 (No. 8555-9201-000, Edition 0810). GEA Westfalia Separator.

[20] Fugarov, D., Purchina, O., Popova, I. and Purchina, A. (2024) Modeling of the Temperature Profile When Heating Fuel Oil with Water Vapor in a Single-Pass Tubular Heat Exchanger. In: Parinov, I.A., *et al.*, Eds., *Physics and Mechanics of New Materials and Their Applications*, Springer, 587-595. https://doi.org/10.1007/978-3-031-52239-0_55

[21] Fonseca, S. (2025) What Does Such a Heating Curve Look like? https://www.autarc.energy/global/knowledge/warmepumpe-heizkurve

[22] Compaore, A., Dianda, B., Nana, G., Bathiebo, D., Zeghmati, B., Chesneau, X., *et al.* (2018) Modeling of Heat Transfer in a Habitat Built in Local Materials in Dry Tropical Climate. *Physical Science International Journal*, **17**, 1-11. https://doi.org/10.9734/psij/2018/38931

[23] Bamogo, K., Ky, T.S.M., Ouédraogo, L.A., Ouédraogo, S., Kam, S. and Bathiebo, D.J. (2025) Conception, Realization and Testing of a Novel Solar Collector. *Solar Energy Advances*, **5**, Article ID: 100107. https://doi.org/10.1016/j.seja.2025.100107

[24] Andrade, E.N.d.C. (1934) XLI. A Theory of the Viscosity of Liquids. Part I. *The London, Edinburgh, and Dublin Philosophical Magazine and Journal of Science*, **17**, 497-511. https://doi.org/10.1080/14786443409462409

[25] Gao, X., Jiang, T. and Li, Y. (2025) A Generalized Model for Estimating the Viscosity of Crude Oil. *Processes*, **13**, Article No. 1433. https://doi.org/10.3390/pr13051433

[26] Ganji, M.J.Z. and Ghassemi, H. (2023) Evaluation of the Solid Particle from Heavy Fuel Oil and Its Formation Trend. *Powder Technology*, **427**, Article ID: 118744. https://doi.org/10.1016/j.powtec.2023.118744

[27] ASTM D93-26 (2026) Standard Test Methods for Flash Point by Pensky-Martens Closed Cup Tester. ASTM International.

[28] Pentax (n.d.) Manuel d'utilisation Pentax HP. ManualsLib, 78. https://www.manualslib.es/manual/428269/Pentax-Hp.html?page=78

[29] Informic (2026) Accelerated Life Testing: Applying the Arrhenius Model in Electronics. https://electroniccomponent.com

[30] WinGD (2025) Operation Manual X82DF. WinGD, 168. https://wingd.com/media/yemj1tfo/om_wingd-x82df-1-0.pdf

[31] Burkina Faso (2016) Arrêté interministériel n˚2016-343/MINEFID/MCIA/MEMC du 13 octobre 2016 portant modalités de fixation du prix de cession des hydrocarbures (DDO, FUEL) pour les centrales thermiques de la SONABEL. Ministère de l'Économie, des Finances et du Développement (MINEFID); Ministère du Commerce, de l'Industrie et de l'Artisanat (MCIA); Ministère de l'Énergie, des Mines et des Carrières (MEMC). Autorité de Régulation du Secteur de l'Énergie (ARSE).